
This is an electronic reprint of the original article.
This reprint may differ from the original in pagination and typographic detail.

Ochoukov, R.; Bilato, R.; Bobkov, V.; Faugel, H.; Kappatou, A.; Schneider, P.; Weiland, M.; Dreval, M.; Sipilä, S.; Dendy, R.; Johnson, T.; Kazakov, Ye; McClements, K. G.; Moseev, D.; Salewski, M.; ASDEX Upgrade Team; EUROfusion Tokamak Exploitation Team

Experimental and numerical investigation of the Doppler-shifted resonance condition for high frequency Alfvén eigenmodes on ASDEX Upgrade

Published in:
Nuclear Fusion

DOI:
[10.1088/1741-4326/ad8762](https://doi.org/10.1088/1741-4326/ad8762)

Published: 01/12/2024

Document Version
Publisher's PDF, also known as Version of record

Published under the following license:
CC BY

Please cite the original version:
Ochoukov, R., Bilato, R., Bobkov, V., Faugel, H., Kappatou, A., Schneider, P., Weiland, M., Dreval, M., Sipilä, S., Dendy, R., Johnson, T., Kazakov, Y., McClements, K. G., Moseev, D., Salewski, M., ASDEX Upgrade Team, & EUROfusion Tokamak Exploitation Team (2024). Experimental and numerical investigation of the Doppler-shifted resonance condition for high frequency Alfvén eigenmodes on ASDEX Upgrade. *Nuclear Fusion*, 64(12), 1-9. Article 126060. <https://doi.org/10.1088/1741-4326/ad8762>

This material is protected by copyright and other intellectual property rights, and duplication or sale of all or part of any of the repository collections is not permitted, except that material may be duplicated by you for your research use or educational purposes in electronic or print form. You must obtain permission for any other use. Electronic or print copies may not be offered, whether for sale or otherwise to anyone who is not an authorised user.

PAPER • OPEN ACCESS

Experimental and numerical investigation of the Doppler-shifted resonance condition for high frequency Alfvén eigenmodes on ASDEX Upgrade















To cite this article: R. Ochoukov *et al* 2024 *Nucl. Fusion* **64** 126060

View the [article online](#) for updates and enhancements.

You may also like

- [Density fluctuation statistics and turbulence spreading at the edge of L-mode plasmas](#)
F.O. Khabanov, R. Hong, P. H. Diamond et al.
- [Experimental research on the TCV tokamak](#)
B.P. Duval, A. Abdolmaleki, M. Agostini et al.
- [Toroidal injection angle dependence of EC assisted plasma initiation at DIII-D](#)
J. Yang, A.C.C. Sips, P. de Vries et al.

Experimental and numerical investigation of the Doppler-shifted resonance condition for high frequency Alfvén eigenmodes on ASDEX Upgrade

R. Ochoukov^{1,*} , R. Bilato¹ , V. Bobkov¹ , H. Faugel¹, A. Kappatou¹ , P. Schneider¹ , M. Weiland¹ , M. Dreval² , S. Sipilä³ , R. Dendy⁴ , T. Johnson⁵ , Ye Kazakov⁶ , K.G. McClements⁷ , D. Moseev⁸ , M. Salewski⁹ , ASDEX Upgrade Team^a and EUROfusion Tokamak Exploitation Team^b

¹ Max Planck Institute for Plasma Physics, Garching, Germany

² Institute of Plasma Physics, National Science Center 'Kharkov Institute of Physics and Technology', Kharkov, Ukraine

³ Department of Applied Physics, Aalto University, Aalto, Finland

⁴ Centre for Fusion, Space and Astrophysics, University of Warwick, Coventry, United Kingdom of Great Britain and Northern Ireland

⁵ Fusion Plasma Physics, Department of Electric Energy Engineering, KTH, Stockholm, Sweden

⁶ Laboratory for Plasma Physics, LPP-ERM/KMS, Brussels, Belgium

⁷ United Kingdom Atomic Energy Authority, Culham Campus, Abingdon, Oxfordshire, United Kingdom of Great Britain and Northern Ireland

⁸ Max Planck Institute for Plasma Physics, Greifswald, Germany

⁹ Department of Physics, Technical University of Denmark, Lyngby, Denmark

E-mail: rochouko@ipp.mpg.de

Received 12 January 2024, revised 10 September 2024

Accepted for publication 16 October 2024

Published 24 October 2024



CrossMark

Abstract

The Doppler-shifted resonance condition for high frequency Alfvénic eigenmodes has been extensively studied on ASDEX Upgrade in the presence of one or a combination of two neutral beam injected (NBI) fast ion populations. In general, only centrally deposited NBI sources drive these modes, while off-axis sources globally stabilize the mode activity. For the case of a single central NBI source, the observed trend is: the highest frequency modes are driven by the lowest energy and lowest pitch angle NBI sources, in line with the expectation from the Doppler-shifted resonance condition. The expected mode frequencies are determined analytically from the two-fluid cold plasma dispersion relation and the most unstable frequency relation, while the mode growth rates are estimated using the fast ion slowing down distribution functions from the ASCOT code. The overall mode frequency trend in a source-to-source

^a See Zohm *et al* 2024 (<https://doi.org/10.1088/1741-4326/ad249d>) for the ASDEX Upgrade Team.

^b See Joffrin *et al* 2024 (<https://doi.org/10.1088/1741-4326/ad2be4>) for the EUROfusion Tokamak Exploitation Team.

* Author to whom any correspondence should be addressed.



Original content from this work may be used under the terms of the [Creative Commons Attribution 4.0 licence](https://creativecommons.org/licenses/by/4.0/). Any further distribution of this work must maintain attribution to the author(s) and the title of the work, journal citation and DOI.

variation is tracked, although a systematic overestimate of ~ 1 MHz is observed. Possible causes of this overestimate include the finite size of the resonant fast ion drift orbit and non-linear effects such as mode sideband formation. Alternatively, the expected mode frequencies are determined by tracking the growth rate maxima trajectories, this method improves the agreement with the experimentally measured values. A combination of two central mode-driving NBI sources results in the suppression of the mode driven by the lowest energy and the lowest pitch angle NBI source. Computing the analytically expected mode frequency following the method outlined above, again, generally tracks the experimentally observed trend. The mode's Alfvénic nature allows for a practical application to track the core hydrogen fraction by following the mode frequency changes in response to a varying ion mass density. Such application is demonstrated in a discharge where the average ion mass is varied from $\sim 2m_p$ to $\sim 1.5m_p$ (where m_p is the proton mass) via a hydrogen puff in a deuterium plasma, in the presence of a strong mode activity. The expected mode frequency changes are computed from the existence of the resonance condition, and the values track the measured results with an offset of ~ 0.5 MHz. Overall, the results suggest an intriguing possibility to monitor and control the D-T ion fraction in the core of a fusion reactor in real time using a non-invasive diagnostic.

Keywords: ASDEX upgrade, Alfvén instability, fast ions, GAE, ICE

(Some figures may appear in colour only in the online journal)

1. Introduction

High frequency Alfvénic modes driven by a single source of fast ions, either neutral beam injected (NBI) or radio frequency (RF)-accelerated, have been extensively documented on multiple tokamaks [1–11]. These observations include results from spherical tokamaks (NSTX [1–3], MAST [3–5], NSTX-U [6]), as well, as standard tokamaks (ASDEX Upgrade [7, 8], DIII-D [9, 10], JT-60U [11]). Spherical tokamak plasmas generally cover the parameter space where the beam ion speed is super-Alfvénic, while beam ions are typically sub-Alfvénic in standard tokamaks. The majority of the experimental studies rely on beam-injected fast ions driven by positive ion sources, which contain three energy components [1–10]. However, these modes are also observed in tokamak plasmas heated by NBI with negative ion sources on JT-60U [11], which have a single energy component. Such results point at a possibility of high frequency Alfvénic mode activity in ITER plasmas, which can then impact the electron heat transport [12, 13].

High frequency modes with a predominantly shear Alfvén polarization are labeled as global Alfvén eigenmodes (GAEs) [14, 15]. GAEs are radially centered in the plasma core near the minimum of the plasma safety factor (q) and extend over a large fraction of the plasma minor radius (r) [14, 15]. Modes with a predominantly compressional polarization are identified as compressional Alfvén eigenmodes (CAEs) and are radially located on the low field side plasma edge [16, 17]. The CAE radial location is determined by the potential well, which is formed via a combination of the radial plasma density profile and the perpendicular mode number $k_\perp \sim r^{-1}$ [16, 17]. In spherical tokamaks, both GAEs and CAEs are commonly excited by the super-Alfvénic beam ions [3]. However, mode stability analysis of plasmas in conventional

tokamaks (ASDEX Upgrade [8], DIII-D [18], JT-60U [11]) shows that GAEs have a consistently larger mode growth rate than CAEs. Theory and simulation can reproduce the experimentally observed frequency and mode number spectra in conventional tokamak plasmas: the modes are counter-current/counter-injection propagating with a fairly high (>10) toroidal mode number and are driven by anisotropy in the fast ion velocity distribution, where the fast ions match the Doppler-shifted cyclotron resonance condition [8, 11, 18–20]. However, these cases generally treat modes driven by a single dominant source of fast ions, where an unambiguous Doppler-shifted resonance condition can be established between the instability frequency, the mode number, and the fast ion drift velocity:

$$\omega - l\omega_{ci} \approx k_\parallel v_\parallel, \quad (1)$$

where ω is the mode frequency, l is the cyclotron resonance coefficient, ω_{ci} is the fast ion cyclotron frequency, k_\parallel is the mode parallel wavenumber, and v_\parallel is the resonant fast ion parallel drift velocity. Only the first cyclotron resonance coefficient is considered ($l = 1$), as higher order modes are generally not observed. Finally, note that an extensive theoretical treatment of the GAE Doppler-shifted resonance condition is provided by Lestz *et al* [21]. However, the results are focused on the spherical tokamak geometry where the fast ions driving the instability are super-Alfvénic by a factor of 3–6 [21], well outside the range found on current conventional tokamaks such as ASDEX Upgrade and DIII-D.

Mode properties under the influence of multiple fast ion sources are not as widely explored. Recent results include discharges on NSTX-U, which demonstrate the mode stabilizing property of tangentially launched off-axis NBI ions [22, 23], and ASDEX Upgrade plasmas, which show the mode

destabilization via RF-accelerated core NBI ions [7, 8]. Prior to NSTX-U, GAE stabilization in the presence of high harmonic fast wave heating has also been observed on NSTX [24]. The results presented in this work focus on modes driven by a combination of two centrally deposited NBI sources, with various pitch angles and injection energies, and, hence, two, possibly distinct, Doppler-shifted resonance conditions. In parallel, we explore the suitability of using an ion cyclotron emission (ICE)-based diagnostic, in the presence of high frequency Alfvénic modes, to track the hydrogen fraction in the core region of tokamak plasmas. Previous theoretical and experimental studies of two-ion effects on high frequency Alfvénic modes include CAEs and ion-ion hybrid modes in a spherical tokamak geometry [25, 26] and shear Alfvén and ion-ion hybrid modes in mirror and tokamak geometries [27, 28]. As the Alfvénic mode frequency is sensitive to the average ion mass density, it allows to map observed frequency changes with changes in the average ion mass and, hence, the hydrogen fraction. In principle, the results can be extrapolated to burning fusion reactors to follow the core tritium fraction in real time.

2. Machine and diagnostics description

This experimental study has been carried out on ASDEX Upgrade, a medium-sized conventional tokamak with a major radius 1.67 m and a minor radius 0.5 m [29]. The machine is capable of operating at on-axis magnetic field values (B_0) of 1.4–3.0 T and at plasma currents (I_p) of 0.4–1.2 MA, as well, as in the reverse I_p/B_0 configurations. The standard B_T and I_p directions are shown in figure 1. Relevant for this study, the machine is equipped with 8 (deuterium) NBI sources at various injection energies and pitch angles, launched via two diametrically opposed ports (figure 1). A detailed view of the NBI source injection geometries, energies, and pitch angles is shown in figure 2. The machine is also equipped with several gas valves capable of injecting deuterium and hydrogen gas species and multiple ICE probes (figure 1). A neutral particle analyzer (NPA) is used for measuring the hydrogen fraction in the plasma core via detection of escaping energetic neutrals [30]. The ICE probes on ASDEX Upgrade use inductors (or B-dot probes) to detect the magnetic field component of fluctuating RF wavefields near the plasma facing wall surfaces [31, 32]. The voltage output from the probe inductors is routed via tri-axial cables directly to Spectrum Instrumentation digitizers, which sample input signals typically at 125 MHz [19].

3. Results and discussion

Frequency spectra of high frequency Alfvénic modes, generated by various single central NBI sources in ASDEX Upgrade deuterium plasmas have already been presented in our previous works, for example in figure 5 in [19] and in figure 7 in [8]. The general trend in the frequency is that the high energy sources (>90 keV, $v_{\text{beam}}/v_A \sim 1.0$ – 1.1 , S5 and S8) produce modes with the lowest frequency, compared to the

low energy sources (<60 keV, $v_{\text{beam}}/v_A \sim 0.8$ – 0.9 , S1–S4) in similar steady-state deuterium target plasmas (figure 3). This trend is in line with the expectations based on matching the Doppler-shifted resonance condition: higher energy fast ions drift at a higher parallel velocity for the injection geometries at ASDEX Upgrade and, thus, require a larger Doppler shift to be in resonance with the mode propagating in the counter-current/counter-injection direction ($k_{\parallel} < 0$). However, we also observe frequency variations between NBI sources of the same energy but different pitch angles. In this case, the trend is to have modes with a higher frequency (and, hence, a smaller Doppler shift) for fast ion sources with lower pitch angle values, which again generally follows the Doppler-shifted resonance condition. Note, that for the case of ASDEX Upgrade it is possible to have multiple energy/pitch angle variations that generate very similar mode frequency values, for example Source 3 (59.3 keV, 0.54 pitch, deuterium) and Source 5 (92.2 keV, 0.43 pitch, deuterium) drive a mode at ~ 6.1 MHz (figure 3(d)). In both cases, the Doppler-shifted resonance condition is met through the variation in the beam ion injection speed and the pitch angle that produces similar parallel fast ion drift velocities. However, in general, we observe that a change in the mode wavenumber (or k_{\parallel}) is also required to match the measured mode frequency values between different NBI sources.

In order to calculate high frequency Alfvénic eigenmode growth rates, we need the fast ion distribution function in the velocity/pitch angle space [34]. This function is obtained for our discharges numerically using a Monte Carlo code, ASCOT [33]. The general procedure for calculating eigenmode growth rates analytically is provided by Lestz *et al* [34] and Belova *et al* [18] and is based on the works of previous authors, referenced in [18, 34]. This analytical approach is linear and treats the plasma as an infinite uniform slab, unlike a realistic bounded tokamak geometry with proper eigenmodes. As a result, the analytical method is only an aid to interpret mode observations. For the convenience of the reader, the integral growth rate equation from [34] is reproduced:

$$\frac{\gamma}{\omega_{ci}} = \frac{\pi}{2} \frac{n_b}{n_e} \sum_l \left| \frac{v_{\parallel, \text{res}, l}^3}{\omega/\omega_{ci0} - l} \right| \int \frac{x J_l^{m\text{-mode}}(\xi)}{(1-x)^2} \left[\left(\frac{l}{\omega/\omega_{ci0}} - 1 \right) \times \frac{\partial f_0}{\partial \chi} + \frac{v}{2} \frac{\partial f_0}{\partial v} \right] d\chi \quad (2)$$

where the equation parameters are defined below. The FLR (finite Larmor radius) function $J_l^{m\text{-mode}}(\xi)$ for cyclotron resonance l and m -mode (=CAE or GAE) is approximated in the limit $0 < \omega/\omega_{ci} < 1$ and the perpendicular wavenumber $k_{\perp} \rightarrow 0$, although nearly the same growth rate results are obtained in the limit $\omega/\omega_{ci} \ll 1$, with a finite $|k_{\perp}| \ll |k_{\parallel}|$. ξ is the FLR parameter ($\xi = k_{\perp} \rho_{\perp b}$, where $\rho_{\perp b}$ is the fast ion Larmor radius), taken in the limit $\xi \ll 1$, consistent with the $|k_{\perp}| \ll |k_{\parallel}|$ approximation. The integration is performed as a function of the trapping parameter χ . This generalized procedure is adapted to the case of ASDEX Upgrade discharges and NBI and is described in [8], where the mode identity is consistent with the

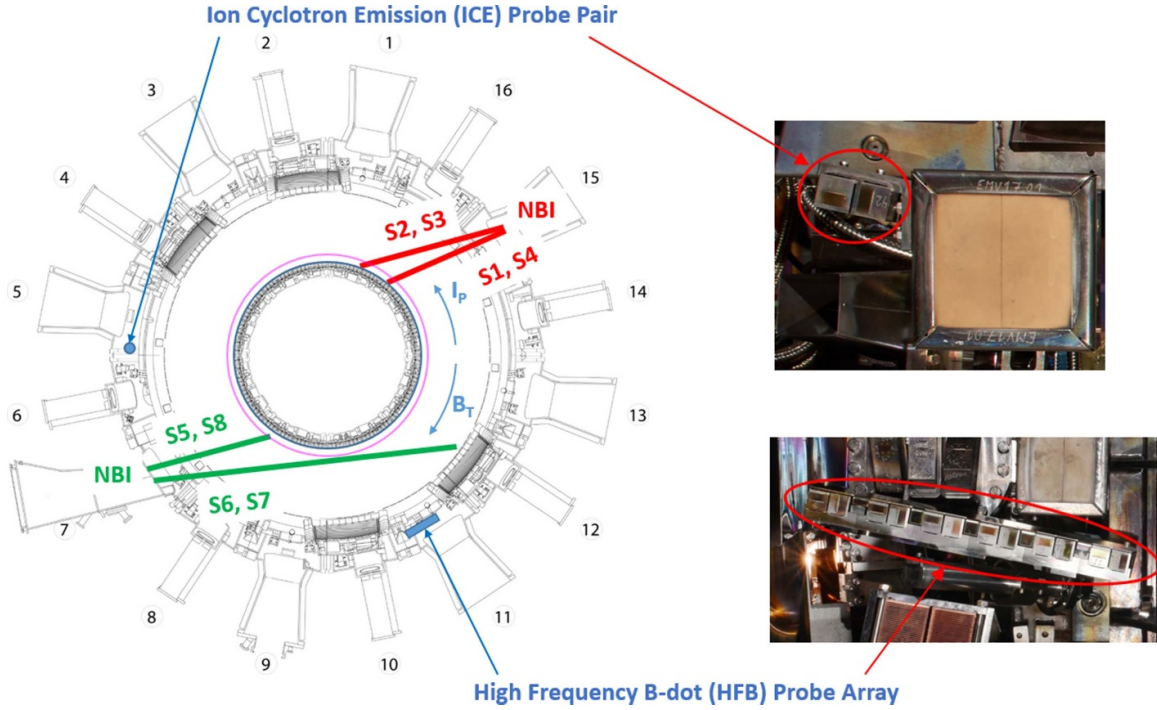


Figure 1. A top cross-sectional view of ASDEX Upgrade. Shown are the standard B_T and I_p directions, the NBI injection geometries, and the in-vessel locations of relevant B-dot probes.

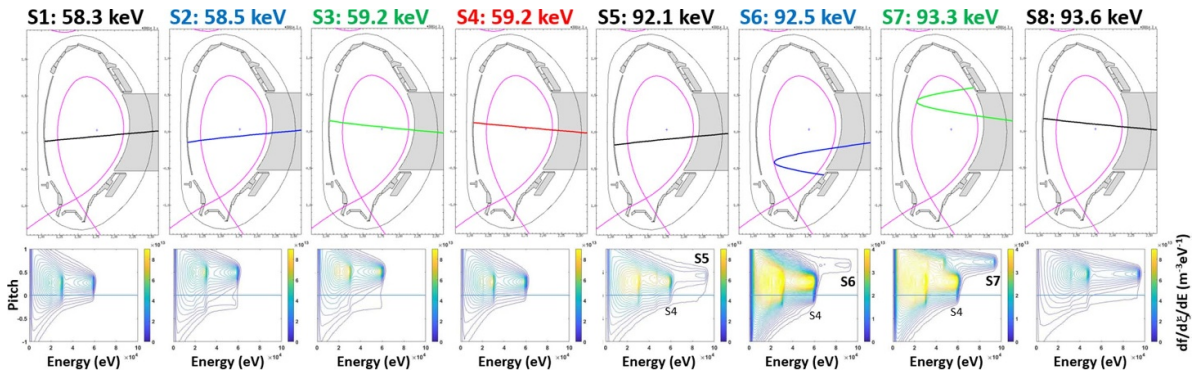


Figure 2. Injection geometry, energy, and pitch distributions of the 8 NBI sources on ASDEX Upgrade. Sources 5, 6 and 7 are shown in combination with Source 4, as they have been used simultaneously for this study. The energy and pitch (ξ) distributions are calculated in the plasma core region using ASCOT [33].

GAE. Following the procedure outlined in [8], on-axis localized growth rate values are estimated for the discharge shown in figures 3(e)–(h), based on the fast ion slowing down distribution function from ASCOT (figure 2). Note that the ASCOT-based estimates include all three beam ion energy (E) components ($E/3$, $E/2$, and full E), unlike the simplified estimates in Lestz *et al* [34], which only account for the full energy beam ion component. In general, about 10% of the mode growth rate value is driven by the $E/2$ component, with the remaining 90% driven by the full E component. To help locate the mode position analytically in the mode number-frequency ($n_{||}$ - f) space, we use the value where the most unstable frequency matches the general Hall-MHD dispersion relation. The equation for the approximate value of the most unstable frequency is:

$$(\omega_{ci} - \omega)^2 = (1 - \chi_o) (k_{||} v_o)^2, \quad (3)$$

where ω_{ci} is the on-axis cyclotron frequency, ω is the mode frequency, χ_o is the trapping parameter, $k_{||}$ is the mode wavenumber and v_o is the fast ion injection speed [18], and is shown by a dashed red curve in figures 4(a)–(e). The limitation of this approximate method is apparent in figures 4(a)–(e) as the dashed red curve often extends into the region with negative growth rate values. The dispersion relation is: $\omega = g k_{||} v_A$, where $g < 1$ is the two-fluid Hall-MHD correction term [18] and v_A is the Alfvén speed, and is shown by a solid black curve in figures 4(a)–(e). The general expression for the correction term g is [18]:

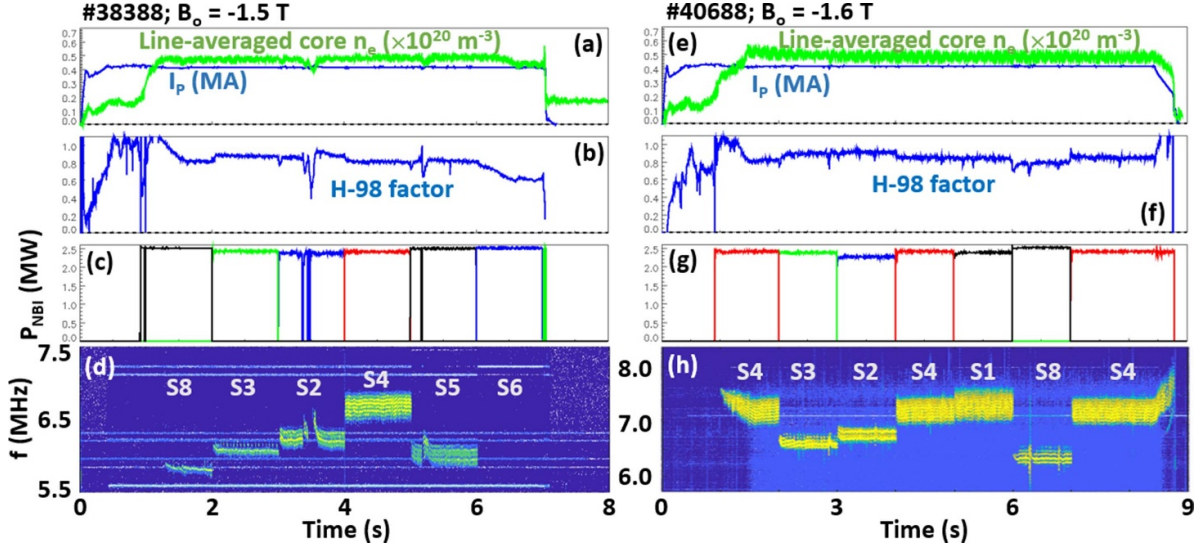


Figure 3. Examples of plasma discharges with high frequency Alfvénic eigenmodes driven by a single NBI source (S1 through S8) at two magnetic field values. Shown quantities are: (a) and (e) the plasma current I_p and the core line-averaged plasma density n_e ; (b) and (f) the H-98 confinement factor; (c) and (g) the NBI power; and (d) and (h) the mode frequency spectra.

$$g^2 = \frac{1}{2} \left[\frac{k^2}{k_{\parallel}^2} (1 + t_{\parallel}^2) + 1 - \sqrt{\left(\frac{k^2}{k_{\parallel}^2} (1 + t_{\parallel}^2) + 1 \right)^2 - 4 \frac{k^2}{k_{\parallel}^2}} \right], \quad (4)$$

where $t_{\parallel} = \frac{k_{\parallel} v_A}{\omega_{ci}}$ is the normalized parallel wavenumber. For the case of ASDEX Upgrade plasmas, where $k_{\parallel} \gg k_{\perp}$, the expression for g simplifies to [18]:

$$g = \sqrt{1 + \left(\frac{t_{\parallel}}{2} \right)^2} - \frac{t_{\parallel}}{2}. \quad (5)$$

The dispersion relation shown by the solid black curves in figures 4(a)–(e) can also be viewed as the location of the Alfvén continuum minimum, since the plasma profile values are taken in the vicinity of q_{\min} . The interception between the two analytical lines is highlighted by orange star symbols and plotted together with the experimental measurements in figure 4(f). The general trend in the estimated mode frequencies for various NBI sources follows the changes in the measured spectra, however, with a consistent overestimate of ~ 1 MHz (figure 4(f)). Several possible explanations that can account for this overestimate are listed below. (1) The finite fast ion drift orbit size is not included in our model and drift orbit averaging would reduce the expected frequency value, i.e. $\langle \omega_{ci} \rangle \approx 0.9 \omega_{ci}$ [34], where the exact correction factor depends on the mode radial dimensions and the radial size of the resonant fast ion drift orbit (figure 4(f)). For simplicity, the on-axis cyclotron frequency value is used throughout this manuscript. (2) The intrinsic inaccuracy of the procedure that locates the most unstable mode value, i.e. the dashed red curve in figures 4(a)–(e), can be responsible for the overestimate of the expected frequency value, and, hence, can be viewed as a rough boundary of the mode driving region [18]. (3) The inability of the simplified linear technique to account for strong

non-linearity such as sideband formation, as observed with the non-linear HYM code in DIII-D discharges [18], is another possibility. An alternative method to locate the expected mode position is by following the growth rate maxima trajectory, as shown by dotted blue lines in figures 4(a)–(e). This method improves the match with the experimentally measured values, compared to the analytical method (circle and star symbols in figure 4(f)); however, it relies on access to a computationally intensive particle code, such as TRANSP or ASCOT, to generate a realistic fast ion velocity distribution function.

Interestingly, a combination of two mode driving (central) NBI sources produces a single high frequency Alfvénic eigenmode (figure 5(d)). A comparison between mode frequency spectra in figure 5(d) and figures 3(d) and (h) reveals that the mode driven by the low energy source (S4, 59.1 keV) with the lowest pitch angle (0.28) becomes suppressed, while the modes driven by high energy (S5 and S8) or high pitch angle source (S2 and S3) remain visible. The mode driven by the low energy and low pitch NBI (S4) fast ions only appears when in combination with another NBI source of a similar energy and pitch angle value (S4 + S1). The two off-axis sources (S6 and S7) completely stabilize the mode activity in the plasma and this observation is in agreement with the results observed on NSTX-U [22, 23]. The mode growth rates for the case of two active NBI sources are calculated following the same procedure as before using the ASCOT code (figure 6).

The resonant growth rate contours reveal that the mode driven by Source 4 becomes suppressed by sources with either higher injection energy or higher pitch angle values (figures 6(a)–(d)). This suppression (or stabilization) is due to the introduction of a stabilizing $d f_0 / d \chi$ region in the fast ion velocity distribution by the additional source. The only exception is the case of S4 + S1, where Source 1 has a similar injection energy and pitch angle value as S4: the mode intensity \sim doubles without a significant change in the mode frequency. Note that the most unstable mode value, i.e. the dashed red

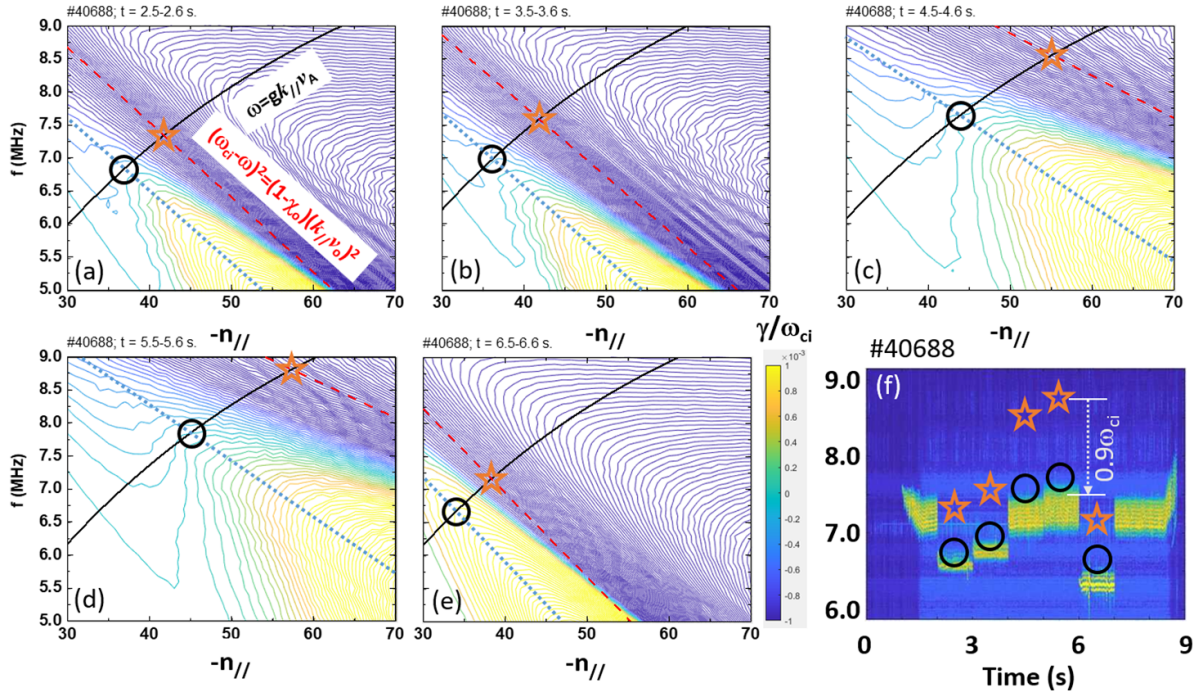


Figure 4. Growth rate values calculated using equation (2) for resonant fast ions, counter-propagating modes ($l = 1$), and the GAE FLR function $J_1^{m\text{-mode}}(\xi)$. The solid black curves in (a)–(e) show the location where both the resonance condition and the GAE two-fluid corrected cold plasma dispersion relation are satisfied. The beam ion sources driving the mode are: (a) Source 3, (b) Source 2, (c) Source 4, (d) Source 1, (e) Source 8. The dashed red lines in (a)–(e) show the expected most unstable frequency, and the dotted blue lines in (a)–(e) show the growth rate maxima trajectories. The orange star symbols show the intersection of the two analytical curves; the black circles show the expected GAE mode locations; the values are plotted together with the experimentally measured values in (f). The white dotted arrow in (f) indicates the expected mode frequency drop from drift-orbit averaging.

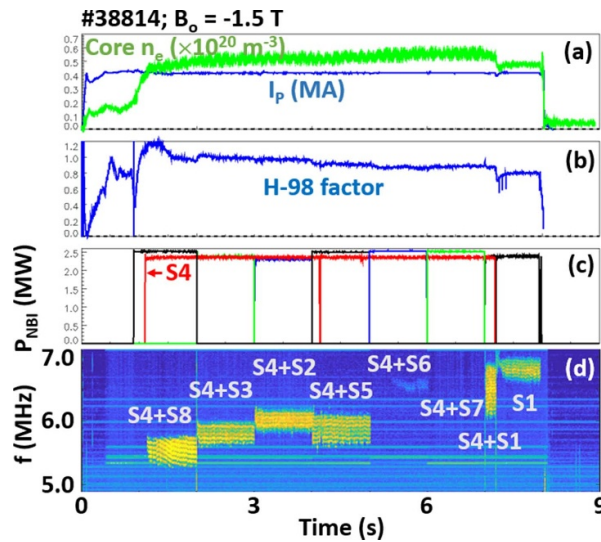


Figure 5. Examples of plasma discharges with high frequency Alfvénic eigenmodes driven by a combination of two NBI sources. Shown quantities are: (a) the plasma current I_p and the core line-averaged plasma density n_e ; (b) the H-98 confinement factor; (c) the NBI power; and (d) the mode frequency spectra. NBI sources S6 and S7 are off-axis and are globally stabilizing.

curve, is calculated using the NBI source with the highest pitch and energy value, out of the two active sources. This choice is based on the empirical observation that the mode driven by the NBI source with a lower pitch becomes suppressed. Comparing the analytically expected mode frequency values

(orange star symbols in figure 6) with actual measurements again reveals a consistent ~ 1 MHz overestimate (figure 6(f)). Tracking the growth rate maxima trajectories, once again, produces an improved match with the experimental values, compared to the analytical method (figure 6(f)).

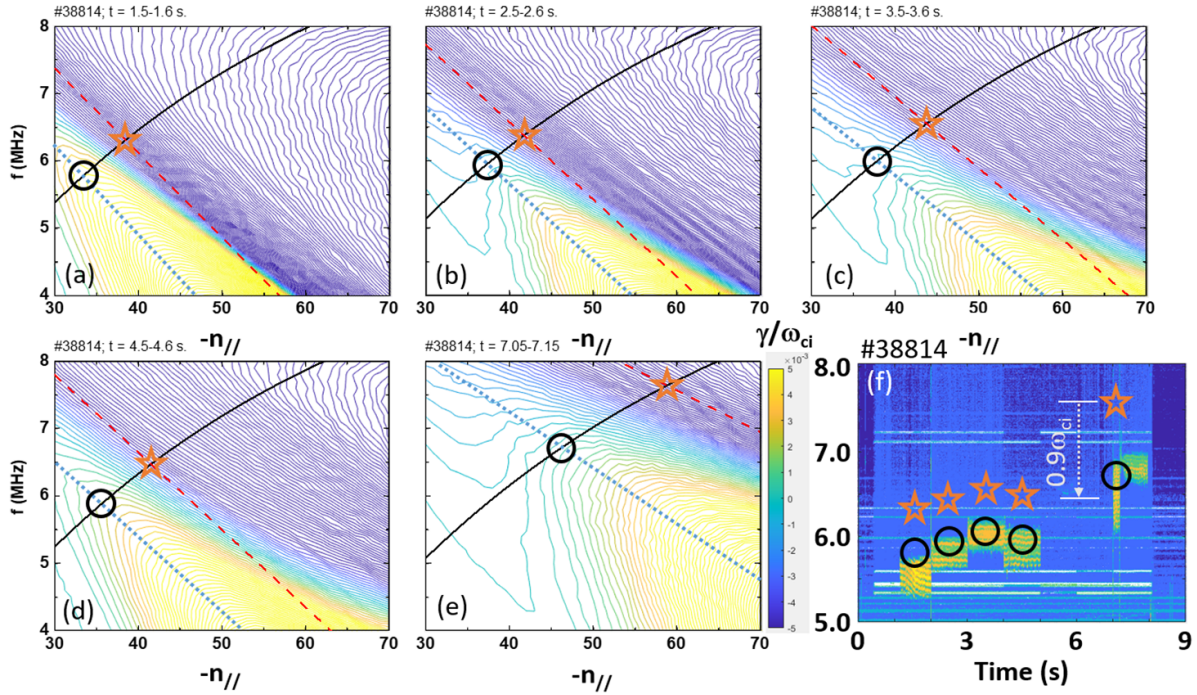


Figure 6. Growth rate values calculated using equation (2) for resonant fast ions, counter-propagating modes ($l = 1$), and the GAE FLR function $J_1^{m\text{-mode}}(\xi)$. The solid black curves in (a)–(e) show the location where both the resonance condition and the GAE two-fluid corrected cold plasma dispersion relation are satisfied. The beam ion sources driving the mode are: (a) Source 4 + Source 8, (b) Source 4 + Source 3, (c) Source 4 + Source 2, (d) Source 4 + Source 5, (e) Source 4 + Source 1. The dashed red lines in (a)–(e) show the expected most unstable frequency, and the dotted blue lines in (a)–(e) show the growth rate maxima trajectories. The orange star symbols show the intersection of the two analytical curves; the black circles show the expected GAE mode locations; the values are plotted together with the experimentally measured values in (f). The white dotted arrow in (f) indicates the expected mode frequency drop from drift-orbit averaging.

The Alfvénic dependence of the mode’s frequency ($f \propto v_A \sim B (m^* n_i)^{-1/2}$) suggests a possibility of using a B-dot probe-based diagnostic to track the average ion mass m^* (or the isotope fraction) in the plasma core. For simplicity, we assume that the electron plasma density is balanced by the bulk ions, with a small contribution from impurities and fast ions that we ignore in making the first estimate: $n_e = n_i \approx n_H + n_D$, or $m^* = (n_H m_H + n_D m_D) n_e^{-1}$, where m^* is the average ion mass. The Alfvén speed can then be calculated as $v_A = B (\mu_0 m^* n_e)^{-1/2}$, where μ_0 is the vacuum permeability. Since it is the mode frequency (and the mode number in the case of a probe array) that we measure, the relation between the frequency and the Alfvén speed is needed. This relation is set by the condition for the existence of the resonance, such as equation (6) in [18]:

$$f/f_{ci} = \omega/\omega_{ci} > (1 + v_o/v_A)^{-1}, \quad (6)$$

where f_{ci} is the cyclotron frequency of the driving fast ion at the mode center. A successful hydrogen fraction scan, in the presence of a strong high frequency Alfvénic mode, has been achieved on ASDEX Upgrade (figure 7). The scan is performed at a constant plasma current, while maintaining the total electron density constant ($\sim 6 \times 10^{19} \text{ m}^{-3}$ on-axis) via a feedback (figure 7(a)). The mode is maintained by a single NBI source at constant power, where the current ramp-up and ramp-down are heated with source 2 (58.5 keV, 0.50 pitch,

deuterium), while the majority of the discharge is heated with source 3 (59.3 keV, 0.53 pitch, deuterium) (figure 7(b)). The hydrogen fraction (which is measured directly by the NPA diagnostic) is scanned almost linearly from the intrinsic value of $\sim 2\%$ to nearly 50%, which lowers the average ion mass from $\sim 2m_p$ (pure deuterium) to $\sim 1.5m_p$ (figure 7(c)). The core electron temperature T_e is ~ 1.5 keV and remains constant during the hydrogen fraction scan. The on-axis magnetic field is also constant at $B_0 = -1.67$ T. The mode frequency increases with a decrease in the average ion mass, as expected from the Alfvén scaling (figure 7(d)). The reader may note that individual sub-modes in figure 7(d) experience non-linear effects (appearance and disappearance) as a function of the average ion mass. The reasons for this behavior are not clear, as both the Alfvén continuum minimum (for the case of the GAEs) and the potential well radial structure (for the case of the CAEs) directly depend on v_A and, hence, the average ion mass. As a result, either mode type can experience a sudden mode number transition due to changes in m^* . Using the average ion mass density values (figure 7(c)), the expected mode frequency values that match the existence of the resonance condition (equation (6) in [18]) can be calculated. These values (on-axis, $R_0 = 1.75$ m) are shown in figure 8. Once again there is an overestimate of ~ 0.5 MHz, compared to the measurement, and a good match to the data can be obtained by using off-axis plasma profiles ($R = 1.84$ m). The exact low field side radial shift value remains to be estimated based on the mode

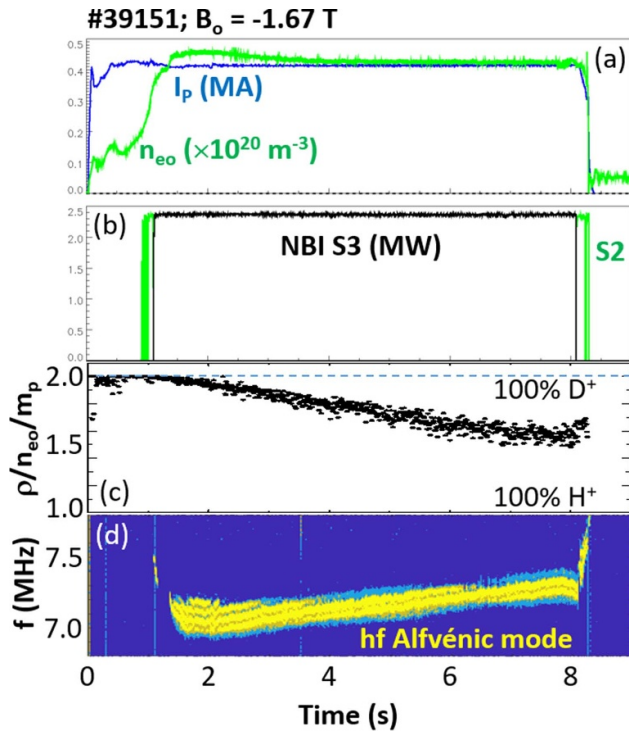


Figure 7. Demonstration of a high frequency Alfvénic eigenmode response to a change in the average bulk ion mass density. Shown are the time histories of (a) the plasma current I_p and the core line-averaged electron density n_{eo} ; (b) the NBI sources and power; (c) the average ion mass density ρ normalized to n_{eo} and the proton mass m_p , as measured with the NPA diagnostic; and (d) the mode frequency spectra.

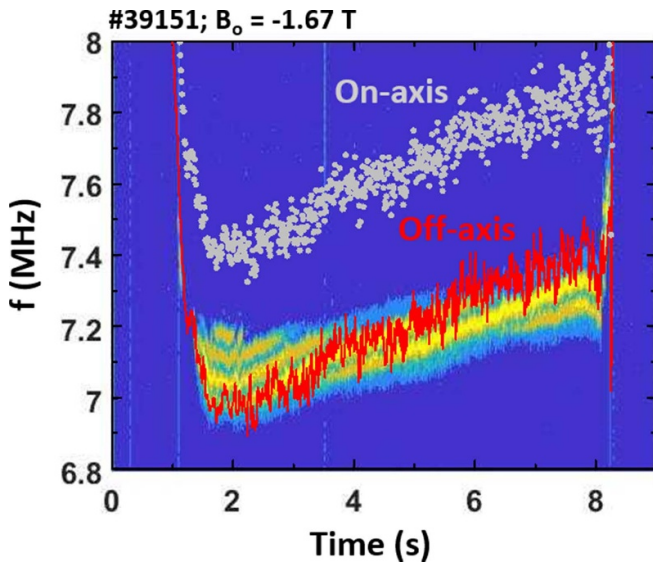


Figure 8. A comparison between a measured high frequency Alfvénic eigenmode frequency and a mode frequency value that matches the existence of the resonance condition. The estimates are performed on-axis ($R_o = 1.75$ m) and off-axis ($R = 1.84$ m).

location and the resonant fast ion drift orbit size. Note that a realistic plasma composition in a fusion reactor will contain additional ion species, such as helium ash and mid-Z radiators,

which will modify the average ion mass density. The effect of impurity ions on the high frequency Alfvénic eigenmode properties is a subject of a future study on ASDEX Upgrade. Additionally note, that other instabilities in the ion cyclotron frequency range, such as core ICE [35], often appear simultaneously in the presence of high frequency Alfvénic modes. As a result, a study that broadly covers multiple instability types and the interplay between them is currently under consideration on ASDEX Upgrade.

4. Summary

Beam driven high frequency Alfvénic eigenmodes are an area of active research on ASDEX Upgrade and other tokamaks. ASDEX Upgrade is well equipped for this study with 8 NBI sources that can inject fast neutrals at energies ranging from <60 to >90 keV and pitch angles from 0.27 to 0.7 (figure 2). The general trends that we report in this manuscript are: (1) centrally depositing NBI sources drive the highest amplitude modes, where the sources with the lowest energy and pitch angle (S1 and S4) produce modes with the highest frequency value (figures 3(d) and (h)); (2) tangentially depositing off-axis NBI sources (S6 and S7) globally stabilize the mode activity (figures 3(d) and 5(d)); (3) a combination of two mode-driving NBI sources (S1–S5, and S8) suppresses the mode associated with the lowest energy and the lowest pitch angle NBI source, while enhancing the amplitude of the mode associated with the remaining source. The mode growth rates in the frequency-mode number space are calculated (figures 4 and 6) following the approach outlined in Lestz *et al* [34] and Belova *et al* [18] and adopted to the ASDEX Upgrade discharges [8]. The mode frequency values are estimated analytically as intersection points between the two-fluid cold plasma dispersion curves and the most unstable frequency curves. It is found that this method, when using on-axis plasma profiles, consistently overestimates the mode frequency by ~ 1 MHz (star symbols in figures 4(f) and 6(f)). This overestimate can possibly be accounted for by (1) using the drift-orbit-averaged cyclotron frequency of the resonant particles, which reduces the on-axis cyclotron frequency values by a factor of ~ 0.9 [34], or (2) using a non-linear model with a realistic tokamak geometry [18], which includes mode sideband formation. The expected mode frequency values are also estimated by tracking the growth rate maxima trajectories and this method improves the match with the experimentally measured frequency values (circle symbols in figures 4(f) and 6(f)).

A successful hydrogen fraction scan has been performed on ASDEX Upgrade in the presence of a strong high frequency Alfvénic eigenmode, where the average bulk ion mass has been scanned from $\sim 2m_p$ (almost pure deuterium) to $\sim 1.5m_p$ ($\sim 50\%$ H/H + D), while keeping the overall electron density constant via a feedback (figure 7). The hydrogen fraction has been measured using the neutral particle analyzer diagnostic. The expected mode frequency change has been estimated using the existence of the resonance condition at on-axis ($R_o = 1.75$ m) and off-axis ($R = 1.84$ m) radial locations (figure 8). The on-axis values show a consistent overestimate

(~ 0.5 MHz) of the mode frequency compared to the measurements, this overestimate is removed for the off-axis radial location. Determining the exact mode position (on-axis vs. off-axis) and the resonant fast ion drift orbit geometry in ASDEX Upgrade discharges will be the subject of future work.

Acknowledgment

This work has been carried out within the framework of the EUROfusion Consortium, funded by the European Union via the Euratom Research and Training Programme (Grant Agreement No 101052200—EUROfusion). Views and opinions expressed are however those of the author(s) only and do not necessarily reflect those of the European Union or the European Commission. Neither the European Union nor the European Commission can be held responsible for them.

The ASCOT-RFOF simulations have been carried out using the Marconi-Fusion supercomputer at CINECA, Bologna, Italy.

ORCID iDs

R. Ochoukov  <https://orcid.org/0000-0002-5936-113X>
 R. Bilato  <https://orcid.org/0000-0002-0578-9333>
 V. Bobkov  <https://orcid.org/0000-0002-2328-9308>
 A. Kappatou  <https://orcid.org/0000-0003-3341-1909>
 P. Schneider  <https://orcid.org/0000-0001-7257-3412>
 M. Weiland  <https://orcid.org/0000-0002-5819-9724>
 M. Dreval  <https://orcid.org/0000-0003-0482-0981>
 S. Sipilä  <https://orcid.org/0000-0002-2748-0601>
 R. Dendy  <https://orcid.org/0009-0002-0017-9103>
 T. Johnson  <https://orcid.org/0000-0002-7142-7103>
 Ye Kazakov  <https://orcid.org/0000-0001-6316-5441>
 K.G. McClements  <https://orcid.org/0000-0002-5162-509X>
 D. Moseev  <https://orcid.org/0000-0001-7955-8565>
 M. Salewski  <https://orcid.org/0000-0002-3699-679X>

References

- [1] Fredrickson E.D. et al 2001 *Phys. Rev. Lett.* **87** 145001
- [2] Gorelenkov N.N., Fredrickson E., Belova E., Cheng C.Z., Gates D., Kaye S. and White R. 2003 *Nucl. Fusion* **43** 228
- [3] McClements K.G. and Fredrickson E.D. 2017 *Plasma Phys. Control. Fusion* **59** 053001
- [4] Sharapov S.E., Lilley M.K., Akers R., Ayed N.B., Ceconello M., Cook J.W.S., Cunningham G. and Verwichte E. 2014 *Phys. Plasmas* **21** 082501
- [5] Appel L.C., Fülöp T., Hole M.J., Smith H.M., Pinches S.D. and Vann R.G.L. 2008 *Plasma Phys. Control. Fusion* **50** 115011
- [6] Fredrickson E.D., Belova E.V., Gorelenkov N.N., Podestà M., Bell R.E., Crocker N.A., Diallo A. and LeBlanc B.P. (the NSTX-U team) 2018 *Nucl. Fusion* **58** 082022
- [7] Ochoukov R. et al (ASDEX Upgrade team) 2020 *Nucl. Fusion* **60** 126043
- [8] Ochoukov R. et al (ASDEX Upgrade Team and EUROfusion MST1 Team) 2023 *Nucl. Fusion* **63** 046001
- [9] Heidbrink W., Fredrickson E.D., Gorelenkov N.N., Rhodes T.L. and Zeeland M.A.V. 2006 *Nucl. Fusion* **46** 324
- [10] Tang S.X., Carter T., Crocker N., Heidbrink W., Lestz J., Pinsker R., Thome K., Van Zeeland M. and Belova E. 2021 *Phys. Rev. Lett.* **126** 155001
- [11] Sumida S., Shinohara K., Ichimura M., Bando T., Bierwage A. and Ide S. 2021 *Nucl. Fusion* **61** 116036
- [12] Stutman D., Delgado-Aparicio L., Gorelenkov N., Finkenthal M., Fredrickson E., Kaye S., Mazzucato E. and Tritz K. 2009 *Phys. Rev. Lett.* **102** 115002
- [13] Ren Y. et al 2017 *Nucl. Fusion* **57** 072002
- [14] Appert K., Gruber R., Troyon F. and Vaclavik J. 1982 *Plasma Phys.* **24** 1147
- [15] Mahajan S.M. and Ross D.W. 1983 *Phys. Fluids* **26** 2195
- [16] Mahajan S.M. and Ross D.W. 1983 *Phys. Fluids* **26** 2561
- [17] Coppi B., Cowley S., Kulsrud R., Detragiache P. and Pegoraro F. 1986 *Phys. Fluids* **29** 4060
- [18] Belova E.V., Crocker N.A., Lestz J.B. and Fredrickson E.D. 2022 *Nucl. Fusion* **62** 106016
- [19] Ochoukov R. et al 2022 *Proc. 24th RF Topical Conf. (Annapolis, USA, 26–28 September 2022)* (<https://doi.org/10.1063/5.0162550>)
- [20] Degrandchamp G.H., Lestz J.B., Van Zeeland M.A., Du X.D., Heidbrink W.W., Thome K.E., Crocker N.A. and Pinsker R.I. 2022 *Nucl. Fusion* **62** 106033
- [21] Lestz J.B., Belova E.V. and Gorelenkov N.N. 2018 *Phys. Plasmas* **25** 042508
- [22] Fredrickson E.D. et al 2017 *Phys. Rev. Lett.* **118** 265001
- [23] Belova E.V., Fredrickson E.D., Lestz J.B. and Crocker N.A. 2019 *Phys. Plasmas* **26** 092507
- [24] Fredrickson E.D., Taylor G., Bertelli N., Darrow D.S., Gorelenkov N., Kramer G., Liu D., Crocker N.A., Kubota S. and White R. 2015 *Nucl. Fusion* **55** 013012
- [25] Lilley M.K. and Sharapov S.E. 2007 *Phys. Plasmas* **14** 082501
- [26] Oliver H.J.C., Sharapov S.E., Akers R., Klimek I. and Ceconello M. 2014 *Plasma Phys. Control. Fusion* **56** 125017
- [27] Farmer W.A. and Morales G.J. 2013 *Phys. Plasmas* **20** 082132
- [28] Farmer W.A. and Morales G.J. 2014 *Phys. Plasmas* **21** 062507
- [29] Zohm H. et al (the EUROfusion Tokamak Exploitation Team and the ASDEX Upgrade Team) 2024 *Nucl. Fusion* **64** 112001
- [30] Schneider P.A., Blank H., Geiger B., Mank K., Martinov S., Ryter F., Weiland M. and Weller A. 2015 *Rev. Sci. Instrum.* **86** 073508
- [31] Ochoukov R., Bobkov V., Faugel H., Fünfgelder H. and Noterdaeme J.-M. 2015 *Rev. Sci. Instrum.* **86** 115112
- [32] Ochoukov R. et al 2017 *Proc. 22nd RF Topical Conf. (Aix-en-Provence, France, 30 May–2 June 2017)* (<https://doi.org/10.1051/epjconf/201715703038>)
- [33] Sipilä S. et al (the ASDEX Upgrade Team and the EUROfusion MST1 Team) 2021 *Nucl. Fusion* **61** 086026
- [34] Lestz J.B., Gorelenkov N.N., Belova E.V., Tang S.X. and Crocker N.A. 2020 *Phys. Plasmas* **27** 022513
- [35] Ochoukov R. et al (ASDEX Upgrade Team and EUROfusion MST1 Team) 2019 *Nucl. Fusion* **59** 086032